Journal of Cellular Biochemistry 104:2348–2362 (2008)

Identification of Genes Regulated by Nanog Which Is Involved in ES Cells Pluripotency and Early Differentiation

Na Liu, Xiaoming Feng, Zhihong Fang, Fengxia Ma, Shihong Lu, Min Lu,* and Zhongchao Han*

State Key Laboratory of Experimental Hematology, National Research Center for Stem Cell Engineering and Technology, Institute of Hematology, Chinese Academy of Medical Sciences and Peking Union Medical College, Tianjin, China

Abstract Nanog plays an important role in embryonic stem (ES) cells pluripotency and self-renewal, yet the precise mechanism through which Nanog accomplishes this important function remains unclear. To understand comprehensive molecular mechanism by which Nanog mediates, we identified genome-wide molecular changes upon silencing Nanog in ES cells by using microarray technology. In order to downregulate Nanog expression efficiently, four siRNAs were designed on the basis of the conserved Nanog sequence and their effects on the Nanog expression were tested. Among these four siRNAs, Nanog-siRNA-P1 was found to be most effective. Once Nanog was downregulated, ES cells underwent differentiation by showing morphological change and decreased proliferation rate. Microarray analysis was then used to identify the altered gene expression after Nanog was silenced. A series of differentially expressed genes due to reduced expression of Nanog was identified as Nanog-related genes. These genes identified here could provide insights into the roles of Nanog in ES cells self-renewal and early differentiation. J. Cell. Biochem. 104: 2348–2362, 2008. © 2008 Wiley-Liss, Inc.

Key words: embryonic stem cells; Nanog; pluripoentcy; microarray; RNA interference

Embryonic stem (ES) cells are derived from the pre-implantation blastocyst. The blastocyst consists of an outer layer of trophoblast cells which give rise to the placenta and an inner cell population called the inner cell mass (ICM). The ICM is destined to give rise to all tissues of the body as well as some extraembryonic tissues, and it is from these cells that ES cells are derived. ES cells have two defining properties, self-renewal and pluripotency, which make them very attractive as an excellent source to therapy of various diseases [Evans and Kaufman, 1981; Smith, 1998; Reubinoff et al., 2000]. In this process, a central step is to develop methods to direct differentiation of ES cells in a controlled manner to produce individual populations of specific cell types. Fully understanding of the mechanism involved in the pluripotency and early differentiation is essential for achieving these goals.

As reported previously, leukemia inhibitory factor (LIF) has been utilized to maintain the symmetrical self-renewal of mouse ES cells [Smith et al., 1988; Williams et al., 1988; Cartwright et al., 2005]. LIF plays an important role in ES cells pluripotency through LIF-STAT3 signaling transduction pathway. STAT3 activation is not only necessary, but also may be sufficient for mouse ES cells self-renewal [Yoshida et al., 1994; Niwa et al., 1998; Matsuda et al., 1999]. But its role is not facultative for human ES cell pluripotency. These results argue that LIF-STAT3 is not fundamental for ES cell pluripotency and predict the existence of other mechanisms involved in both human and mouse ES cells pluripotency [Daheron et al.,

This article contains supplementary material, which may be viewed at the Journal of Cellular Biochemistry website at http://www.interscience.wiley.com/jpages/0730-2312/suppmat/index.html.

Grant sponsor: National Natural Science Foundation of China; Grant numbers: 30570357, 30600238; Grant sponsor: Tianjin Municipal Science and Technology Commission; Grant numbers: 06YFSZSF01300, 05YFJZJC01500.

*Correspondence to: Zhongchao Han or Min Lu, Institute of Hematology, Chinese Academy of Medical Sciences & Peking Union Medical College, Tianjin 300020, China.
E-mail: tihzchan@public.tpt.tj.cn; minlu001@yahoo.com

Received 4 January 2008; Accepted 26 March 2008
DOI 10.1002/jcb.21795

© 2008 Wiley-Liss, Inc.

2004]. Recently, several groups of researchers have identified some crucial factors involve in ES cells self-renewal, such as Nanog [Chambers et al., 2003; Mitsui et al., 2003], Oct4 [Nichols et al., 1998; Niwa et al., 2000], Sox2 [Avilion et al., 2003], and Klf4 [Li et al., 2005a]. Besides of these factors, ERK [Hamazaki et al., 2006; Li et al., 2007], Wnt [Kielman et al., 2002; Sato et al., 2004; Miyabayashi et al., 2007], PI3K [Paling et al., 2004; Watanabe et al., 2006] and TGFβ [Ying et al., 2003; Liu et al., 2007] signaling pathways have also been shown to play a role in ES cells self-renewal.

Nanog, a homeodomain-containing protein, is identified as a crucial factor that could sustain ES cells pluripotency even in the absence of LIF [Chambers et al., 2003; Mitsui et al., 2003]. Nanog is specifically expressed in ES cells and is rapidly downregulated during differentiation. Nanog is originally proposed as a transcription repressor to inhibit the expression of genes important for cell differentiation [Pan and Pei, 2005]. ES cells lacking Nanog trend to differentiate spontaneously even in the presence of LIF. RNA interference (RNAi)-mediated knockdown of Nanog lead to differentiation of both mouse and human ES cells [Zaehres et al., 2005; Ivanova et al., 2006]. Overexpression of Nanog in mouse and human ES cells enables them to undergo self-renewal in the absence of LIF and feeder cells [Chambers et al., 2003; Mitsui et al., 2003; Darr et al., 2006]. Nanog-overexpressing mouse ES cells also show a marked increase in reprogramming activity after fusion with neural stem cells [Silva et al., 2006]. Takahashi and his colleague generated induced pluripotent stem (iPS) cells from mouse embryonic fibroblasts by introducing four factors, Oct4, Sox2, c-Myc and Klf4 [Takahashi and Yamanaka, 2006; Takahashi et al., 2007]. Very recently, three groups generate iPS cells using Nanog as a more stringent selection marker. Nanog-selected iPS cells are almost indistinguishable from ES cells derived from ICM [Okita et al., 2007; Meissner et al., 2007; Wernig et al., 2007]. A just published report showed that four factors (Oct4, Sox2, Nanog, and Lin28) are sufficient to reprogram human somatic cells to pluripotent stem cells that exhibit the essential characteristics of ES cells [Yu et al., 2007]. Although all of these evidences show Nanog is a key transcription factor in ES cells self-renewal, the specific genes regulated by this factor in ES cells have not been well identified. Elucidating the target genes of Nanog can help us to study the mechanism of ES cells self-renewal and differentiation, and it will be helpful to generate specific cell lineage which can be used in clinic.

In this article, we aimed to investigate the genes regulated by Nanog in order to determine the role of Nanog in the regulation of ES cells self-renewal. For this purpose, it was important to manuscript the expression level of Nanog in ES cells. Here, we knocked down Nanog expression in mouse ES cells by RNA interference (RNAi)-mediated gene silencing. Microarray analysis was then used to identify the downstream genes of Nanog. In this case, we chose the earliest time when ES cells just lose their Nanog expression. These genes identified here will provide insights into the roles of Nanog in ES cells self-renewal and early differentiation.

MATERIALS AND METHODS

Mouse ES Cell Culture

Mouse ES cell line, J1 cell line, was derived from a male agouti 129S4/SvJae embryo [Li et al., 1992]. J1 cells (kindly provided by Dr. Zhengyu Wang (Harvard University)), were cultured, as previously reported by our laboratory [Li et al., 2005b], on γ-irradiated mouse embryonic fibroblast feeder layer (SNL). The medium consisted of high glucose Dulbecco's Modified Eagle Medium (DMEM) (no-pyruvate, high-glucose formulation; GIBCO-BRL) supplemented with 15% fetal bovine serum (Hyclone); 1× nonessential amino acids (Hyclone), 2.0 mM L-glutamine, 1000 U/ml mouse recombine LIF (Chemicon); 100 μM 2-mercaptoethanol (Sigma), 100 U penicillin; and 100 μg/μl streptomycin. The culture medium was changed every day, and the cells were passaged every 2 or 3 days. Differentiated J1 cells were induced by removing LIF and SNL from culture medium for 7 days. SNL was cultured in the DMEM with 10% fetal bovine serum, 2 mM L-glutamine, 100 U penicillin, and 100 μg/μl streptomycin.

siRNAs Design, Synthesis and Transfection

Four siRNAs corresponding to Nanog (AY278951.1) were designed as recommended [Elbashir et al., 2002] (using the Ambion online designer tools at http://www.ambion.com/techlib/misc/sirna_tools.html). In brief, we selected siRNA sequence that started with AA and then analyzed every sequence by BLAST (http://www.ncbi.nlm.nih.gov/blast) to ensure

that there were no significant sequence homologies with other genes. Four siRNA sequences for Nanog were selected for testing. GFP-siRNA served as negative control siRNA which lacks significant sequence homology to the genome. And the duplex siRNA was synthesis by the Silencer siRNA Construction Kit (Ambion). Mouse Nanog short interference and negative control siRNA sequences are listed in Table I. Cy3-labeled siRNAs were synthesized using Label IT siRNA Tracker Intracellular Localization Kit (Mirus). Cy3-labeled GFP-siRNA allows to visual monitoring of transfection efficiency. After 24 h, transfection efficiency was counted by flow cytometry.

All transfections were done using Lipofectamine 2000 (Invitrogen) according to the standard protocol. To increase transfection efficiency cells were transfected at the time of plating. J1 cells were seeded onto 24-well plates at 10^5 cells per well and transfected with 100 nM siRNA with 2 μg/ml Lipofectamine 2000. siRNA duplex and Lipofectamine 2000 were diluted with opti-DMEM. Each knockdown experiment was performed at least twice.

RNA Extraction

At 24 and 48 h after transfection, total RNA was isolated by the TRIzol method (Invitrogen) according to the manufacturer's protocol. Twenty micrograms total RNA was purified using RNeasy Mini-Kit (Qiagen) following the manufacturer's RNA clean-up protocol with the optional on-column DNase treatment. The integrity and quality of the RNA were verified by electrophoresis and its concentration was measured. Two micrograms total RNA was reverse transcribed using M-MLV reverse transcriptase (Promega) in 50 μl volume at 37°C for 2 h.

Polymerase Chain Reactions Analysis of Gene Expression

Polymerase chain reactions (PCRs) were carried out using Taq DNA polymerase (TaKaRa, Japan). Primers for RT-PCR and real-time PCR were obtained from Sangon (Shanghai). Real-time PCR analysis was carried out using QuantiTect SYBR Green PCR Master mix (Qiagen). PCR reactions were carried out in an ABI7500 sequence detection system (Applied Biosystems, CA) as follows: 95°C for 15 min for 1 cycle and 40 cycles of 94°C for 15 s and 60°C 30 s and 72°C 34 s. A dissociation curve was run at the

TABLE I. Sequence Information About Nanog siRNAs and Negative Control siRNA

dsRNAs	Target sequence	Sense and antisense sequence for synthesis
Nanog-siRNA-P1	AAGGACAGGTTTCAGAAGCAG	5-AAGGACAGGTTTCAGAAGCAGCCTGTCTC-3; 5-AACTGCTTCTGAAACCTGTCCCTGTCTC-3
Nanog-siRNA-P2	AAGACCTGGTTTCAAAACCAA	5-AAGACCTGGTTTCAAAACCAACCTGTCTC-3; 5-AATTGGTTTTGAAACCAGGTCCCTGTCTC-3
Nanog-siRNA-P3	AATGCTGCTCCGCTCCATAAC	5-AATGCTGCTCCGCTCCATAACCCTGTCTC-3; 5-AAGTTATGGAGCGGAGCAGCACCTGTCTC-3
Nanog-siRNA-P4	AATTTGGAAGCCACTAGGGAA	5-AATTTGGAAGCCACTAGGGAACCTGTCTC-3; 5-AATTCCCTAGTGGCTTCCAAACCTGTCTC-3
GFP-siRNA	AAGAGCGATTTGGACGACAAG	5-AAGAGCGATTTGGACGACAAGCCTGTCTC-3; 5-AACTTGTCGTCCAAATCGCTCCCTGTCTC-3

end of the reaction for product specificity. For each sample, expression of target and marker genes was normalized to the expression of GAPDH. The primers used for real-time PCR were shown in supplemental online Table I. Each real-time PCR reaction was performed in duplicate.

Flow Cytometry

J1 cells were dissociated with Trypsin (0.25%) plus EDTA (1 mM, GIBCO), washed twice in phosphate-buffered saline (PBS). The cells were then immediately analyzed on a FACScan flow cytometer (Becton Dickinson).

Western Blotting

Cells were collected and washed twice with cold PBS. And then cells were resuspended in cell lysis buffer containing 50 mM Tris (pH 7.4), 150 mM NaCl, 1 mM EDTA, 1 mM EGTA, 1 mM NaF, 20 mM $Na_4P_2O_7$, 1 mM Na_3VO_4, 1% Triton X-100, 10% glycerol, 0.25% deoxycholate and 0.1% SDS. Lysate was electrophoresed using SDS-PAGE (10% polyacrylamide gel) and blotted 1.5 h onto polyvinylidene difluoride (PVDF) membrane. Membranes were blocked for overnight with 5% fat-free milk solution. Samples were probed with antibody anti-Nanog 1/1,000 (BETHYL) and anti-actin 1/200 (Santa Cruz Biotechnology). Anti-goat or anti-mouse IgG-peroxidase conjugate (Sigma) was diluted at 1:5,000. Staining was visualized using an electogenerated chemiluminescence (ECL) kit (Amersham Biosciences Corp.).

Cell Proliferation Assays

Cell counts. J1 cells were seeded in gelatin-coated six-well plates at a density of 3×10^4 cells per well and then transfected with Nanog-siRNA-P1 and GFP-siRNA at 100 nM. Triplicate wells for each treatment. And cells were digested using 0.25% trypsin–EDTA at 12, 24 and 48 h after transfection. Trypan blue was added to the suspension and the number of viable (Trypan blue negative) cells was counted using a hemocytometer.

Cell proliferation was measured using Cell Proliferation ELISA, BrdU (Roche Molecular Biochemicals). We measured BrdU incorporation according to the manufacturer's protocol. J1 cells were cultured on gelatin in 96-well plates (10^4 cells/well) with or without Nanog RNA interference. At 45 h after transfection, BrdU was added to a final concentration of 10 μM. Cells were labeled with BrdU for 3 h. After fixation, a peroxidase conjugated anti-BrdU antibody was added and incubated for 60 min after washing, a peroxidase substrate was added and absorbance was measured in an ELISA plate reader. Data were analyzed by Student's t-test. A value of $P < 0.05$ was considered statistical significance.

Microarray Analysis

According to the methods previously described [Patterson et al., 2006], microarray analysis was performed in CapitalBio Corp. (Beijing, China) using 36K Mouse Genome Array (version 4.0), consisting of 35,852 70-mer probes representing 25,000 genes and 38,000 gene transcripts, was purchased (Operon) and printed on silanized glass slides using a SmartArray™ microarrayer (CapitalBio). Five micrograms DNase-treated total RNA was prepared and fluorescent dye (Cy5 and Cy3-dCTP)-labeled cDNA, produced through Eberwine's linear RNA amplification method [Van Gelder et al., 1990] and subsequent enzymatic reaction, were then hybridized to an array. Finally, arrays were scanned with a confocal LuxScan™ scanner (CapitalBio), and the data of obtained images were extracted with SpotData software (CapitalBio).

After normalized by the LOWESS method, the data were filtered for nonreliable signals [Yang et al., 2002]. Significantly different genes were identified using a 1-class unpaired significance analysis of microarrays (SAMs) [Tusher et al., 2001]. The SAM delta values were adjusted to obtain the largest gene list that gave a false discovery rate (FDR) of less than 5%. Using the SAM-derived gene lists, average linkage hierarchical cluster analysis was conducted using Pearson correlation in the Cluster program and the data were visualized in Treeview [Eisen et al., 1998].

RESULTS

Silencing of Nanog Expression by RNA Interference

In order to knock-down endogenous Nanog expression effectively in J1 cells, we initially tested four different siRNAs directed against Nanog mRNA. The mouse Nanog gene and the location of the four siRNAs target sites are indicated in Figure 1A. The sequence information is listed in Table I. We labeled GFP-siRNA with Cy3 to analyze the transfection efficiency

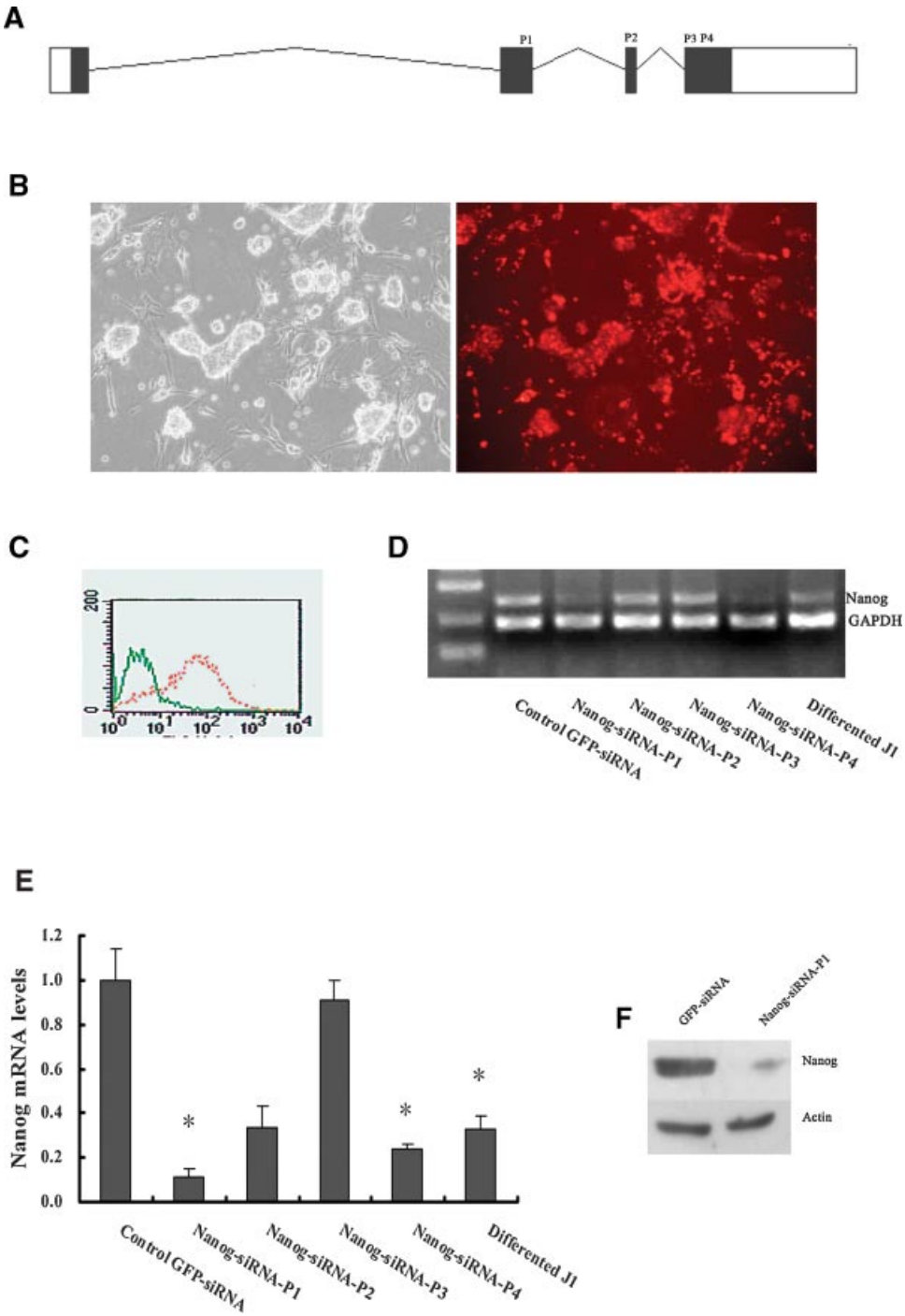

Fig. 1. Nanog RNA interference specifically reduces Nanog expression in J1 cell line. **A**: Schematic representation of the mouse Nanog gene; exons are represented by boxes and introns by lines. The location of four siRNAs target sites is indicated. **B**: Visualization analysis of transfection efficiency of siRNA in J1 cells. Photos were taken at 24 h after Cy3-GFP-siRNA was transfected. **C**: Flow cytometry analysis of transfection efficiency at 24 h. Cells were seed in 24-well plates, and transfection was performed as described in materials and methods. The transfection efficiency was up to 93% when J1 cells were transfected with 100 nM Cy3-GFP-siRNA. **D**: RT-PCR analysis. Total RNA was extracted from cells treated for 24 h with the siRNAs against Nanog or with siRNA against GFP. GADPH was used as an internal control. Molecular weight markers are indicated on the left. **E**: Nanog expression was assessed by real-time PCR 24 h after transfection in cells treated with Nanog-siRNAs and GFP-siRNA. Differentiated J1 cells were used as a positive control. The data were represented the mean $\pm$ SD from three independent experiments. The value for the GFP-siRNA treated cells was set to 1 (100%), and all other values were calculated with respect to this. Statistical significance of the results was assessed using Student's *t*-test. *Statistically significant changes in expression between the Nanog siRNA treated cells and control cells ($P < 0.01$). **F**: Western blot analysis of Nanog protein levels in J1 cells 24 h after transfection. The blot was probed with antibodies against Nanog and beta-Actin. [Color figure can be viewed in the online issue, which is available at www.interscience.wiley.com.]

of siRNA in J1 cells. GFP-siRNA-Cy3 was transfected in J1 cells as described in methods. Strong intracellular fluorescent signal was observed by fluorescence microscopy in each J1 cells colony at 24 h after transfection (Fig. 1B). Ninety-three percent of transfection efficiency was determined by flow cytometry analysis (Fig. 1C), which was sufficient for our RNAi experiment.

Following establishment of the improved transfection method for J1 cells, we proceeded to transfect J1 cells using siRNAs and measured Nanog mRNA levels to identify the effective siRNA for Nanog silencing. We used the optimized transfection condition established in previous experiment. Differentiated J1 cells were used here as positive control cells in which Nanog expression was downregulated. As shown in Figure 1D, transfection of each of four different Nanog-siRNAs into J1 cells resulted in a reduction of endogenous Nanog mRNA to different levels. Nanog-siRNA-P2, Nanog-siRNA-P3 and GFP-siRNA did not show significant downregulation of Nanog at concentrations up to 100 nM. The precise interference rate at mRNA level was then analyzed by real-time PCR. We consistently observed the strongest inhibitory effect on Nanog expression by Nanog-siRNA-P1 (Fig. 1E). Nanog-siRNA-P1 reduced Nanog expression significantly: the level is only 11% of that of the GFP-siRNA control. Nanog expression level in J1 cells treated with Nanog-siRNA-P1 was even lower than that in the differentiated J1 cells. This result showed Nanog-siRNA-P1 could efficiently silence Nanog expression. Efficiency of Nanog silencing was also confirmed by analyzing Nanog protein level (Fig. 1F). Therefore, we chose Nanog-siRNA-P1 for subsequent analyses.

Morphological Change of ES Cells after Nanog-Silencing

To explore the effect of Nanog downregulation in mouse ES cells, we examined the phenotype change of cells after Nanog-silencing. At 24 h after transfection, it had no obvious difference between the Nanog downregulated and control cells. Forty-eight hours after transfection, untreated ES cells (Fig. 2A) and GFP-siRNA control (Fig. 2B) cells maintained the undifferentiated morphology. Cells grew as compact colonies. However, the Nanog downregulated cells lost the compact dome-like colony morphology

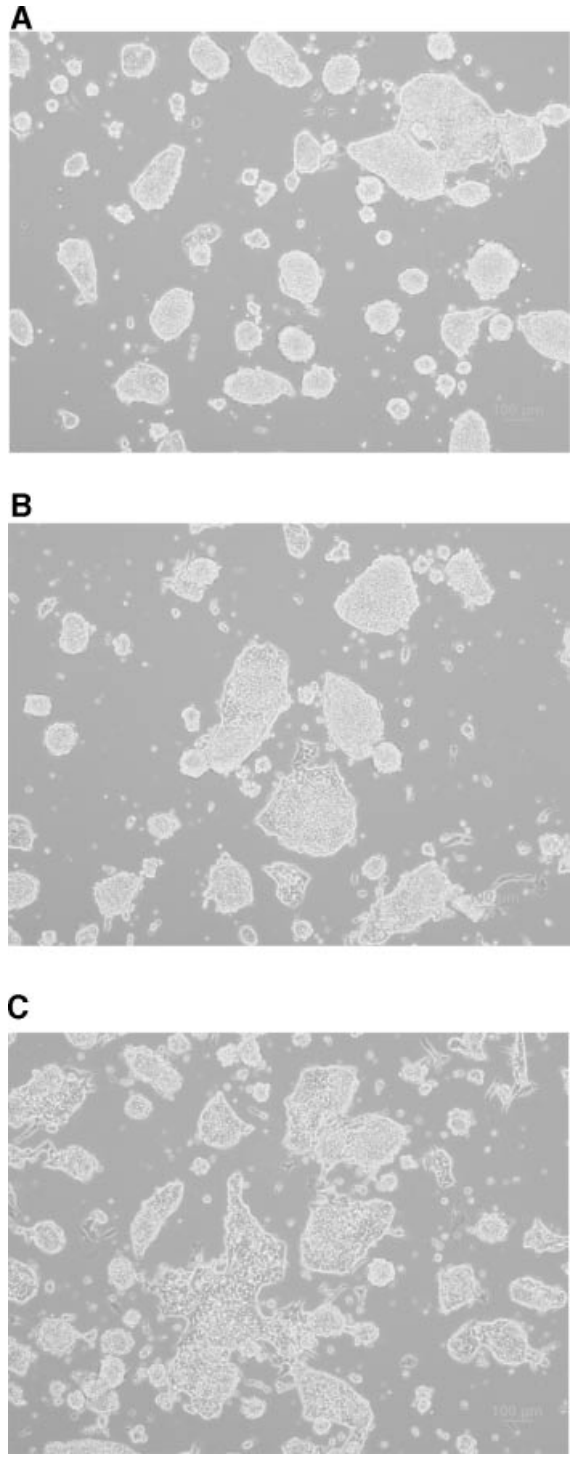

Fig. 2. J1 cells phenotype after Nanog was knockdown. Pictures were taken 48 h after transfection. Untreated cells (**A**) and GFP-siRNA transfection cells (**B**) maintain ES cells compact colony morphology. **C**: Cells transfected with Nanog-siRNA-P1 displayed differentiated phenotype. Cell colony became flat and spread.

characteristic of undifferentiated cells and assumed the morphology of differentiated cells, exhibiting highly spread and an expansive cytoplasm that frequently surrounded neighboring cells (Fig. 2C). This result indicated that Nanog was a crucial factor in ES cells pluripotency, whose downregulation induces ES cells differentiation even in the presence of LIF [Chambers et al., 2003; Mitsui et al., 2003].

Inhibition of J1 Cell Growth by Downregulation of Nanog Expression

In the RNA interference experiment, we found J1 cells colonies in Nanog downregulated group were smaller than that of control group. We continued to examine if Nanog downregulation could affect J1 cells proliferation. We seed J1 cells in 6 wells plate at concentration of 3×10^4 cells/well, and counted the number of cells at 12, 24, 48 h after Nanog-siRNA-P1 transfection. Each treatment performed triplicate. The results showed that knock-down of Nanog impaired cell proliferation. Nanog downregulation significantly inhibited J1 cells growth at 48 h (Fig. 3A).

BrdU incorporation assay was then used to confirm the effects of Nanog-siRNA-P1 on J1 cells proliferation as previously assessed by cell count assay. The BrdU assay measures incorporation of BrdU in cell DNA which correlates with DNA synthesis and allows a direct evaluation of cell proliferation on DNA level. It measures cell proliferation by detecting dividing cells. Similar to the results of cell count assay, BrdU incorporation of GFP-siRNA treated control cells and untreated cells did not differ significantly, indicating that the RNA interference process has no effect on cell proliferation. BrdU incorporation in Nanog-siRNA-P1 treated cells was significantly lower than that of the untreated cells and control cells (Fig. 3B).

Identification of Genes That Differentially Expressed After Silencing of Nanog Expression

To identify Nanog-related genes, we suppressed Nanog expression in mouse ES cells using Nanog-siRNA-P1 and analyzed the resulting alteration of the expressed gene profile with a microarray system. Changes in the expression pattern of cellular genes were analyzed 24 and 48 h after transfection (in triplicate). SAM, a statistical method adapted specifically for microarrays, was used to identify

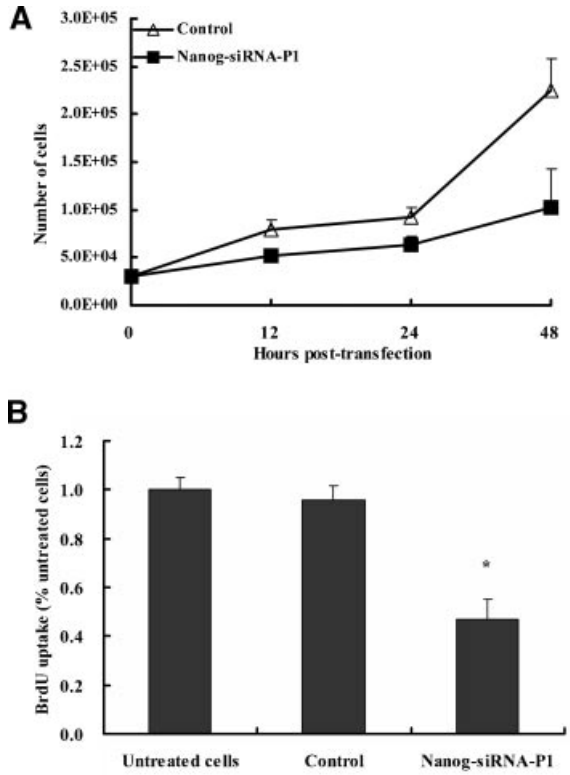

Fig. 3. Cell growth inhibition by Nanog-silencing in J1 cells. **A**: 3×10^4 cells were seeded on a six-well flask and cultured for 3 days. Cell growth rate was performed in triplicate and quantified by counting cells under light microscopy at an indicated time after transfected. **B**: Cell viability was determined by BrdU assay at 48 h after transfection. Cell viability is significantly decreased in J1 cells undergoing Nanog knock-down. Bar graphs represent mean ± SD, N = 8. $^*P < 0.01$ vs. control cells.

genes that were differentially expressed between the J1 cells transfected with Nanog-siRNA-P1 and GFP-siRNA [Tusher et al., 2001]. GFP-siRNA served to correct for potential off-target effects that could be induced by siRNAs in general [Cullen, 2006]. We only selected genes that fulfilled the cut-off criteria of an FDR <5% for further analysis. Using this method, 1,169 and 1,242 genes were identified as differentially expressed at 24 and 48 h after Nanog was downregulated (Fig. 4C). Two thousand six genes were identified at least at one time and 395 genes expression was changed at both time points. The genes with significant change are presented in supplemental online data Table II. These differentially expressed genes were then grouped according to their expression profile by hierarchical clustering with the Pearson's correlation (Fig. 4). Figure 4A shows that the pattern of gene

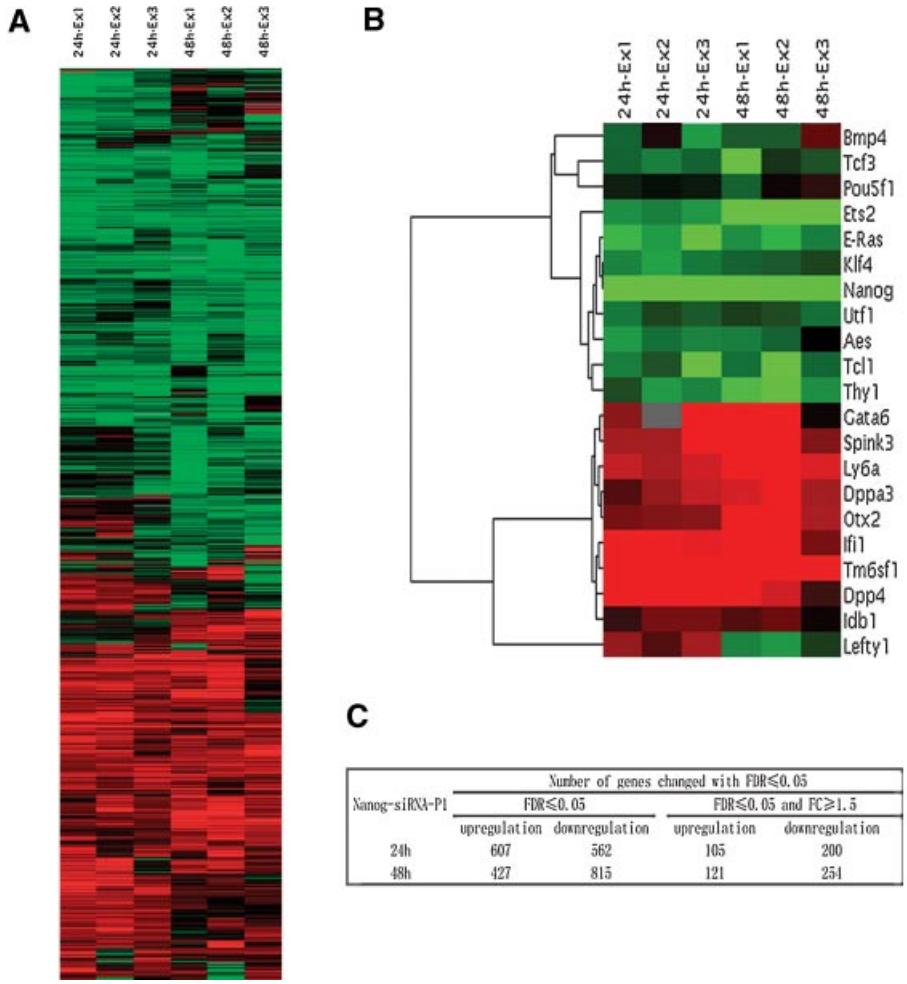

Nanog-siRNA-P1	Number of genes changed with FDR≤0.05			
	FDR≤0.05		FDR≤0.05 and FC≥1.5	
	upregulation	downregulation	upregulation	downregulation
24h	607	562	105	200
48h	427	815	121	254

Fig. 4. Heatmap of differentially expressed genes upon siRNA-mediated silencing of Nanog expression. **A**: Genes which were changed with FDR < 0.05 in any of the two time points were hierarchical clustered for similarity. **B**L Examples of genes with significant change at both 24 and 48 h (FDR < 0.05). Color code: red, upregulation; green, downregulation, black, no change; gray, absent. **C**: Number of genes with significantly different expression following Nanog loss. [Color figure can be viewed in the online issue, which is available at www.interscience.wiley.com.]

expression at 48 h was similar to that at 24 h. The top 30 statistically significant up- and downregulated genes at each time points after Nanog silenced were listed in Figure 5.

Nanog downregulation could induce ES cells differentiation. And more gene expression would be altered during ES cells differentiation. Those genes included differentiation-related and Nanog-related genes. In order to well explore the Nanog-related genes rather than differentiation-related genes, our focus presently concentrates on these genes whose expression was changed at the earlier time point (24 h) when Nanog was downregulated. By adopting this approach, we identified a subset of 1,169 genes (FDR < 0.05) as Nanog-related genes including 607 upregulated and 562 downregulated genes in Nanog-silencing J1 cells (supplemental online data Table II). A significant subset of outlier genes were further narrowed by filtering genes that showed a great than ±1.5-fold expression change in Nanog-silencing J1 cells compared to the average values for control cells. From this analysis 305 genes were identified (Fig. 4C).

Results revealed some genes involved in ES cells self-renewal and pluripotency were downregulated after Nanog-silencing, such as Utf1, Tcl1, Tcf3, Klf4, Aes1, Thy1, and Ets2 [Li et al., 2005; Ivanova et al. 2006; Matoba et al. 2006; Pereira et al., 2006; Takahashi and Yamanaka, 2006; Tan et al., 2007]. On the other hand, some genes implicated in differentiation were upregulated, including Lefty1, Otx2, GATA6

A Nanog-siRNA vs GFP-siRNA

Gene	Q value (%)	Fold
D12Ertd647e	2.586	3.4
Ap3b2	2.761	2.9
Slc16a14	2.586	2.8
Tm6sf1	0.000	2.6
Sms	0.000	2.5
Max	3.148	2.4
Dpp4	0.000	2.4
Irgm	0.000	2.1
Dffa	0.000	2.0
Gbp4	0.191	2.0
Nphs1	0.000	2.0
Sys6	0.000	2.0
Oas2	0.659	2.0
Nras	0.724	2.0
Vdac1	3.426	2.0
Rnf32	1.049	2.0
Plekhc1	0.000	1.9
Q8BR24	2.961	1.9
Q9D3E4	2.761	1.9
Podxl	0.000	1.9
Wrb	0.000	1.9
Zbp1	0.191	1.9
Gadd45a	0.000	1.8
Ccl5	2.761	1.8
Minpp1	3.965	1.8
Rab3il1	1.198	1.8
Adfp	0.000	1.7
Rtp4	3.495	1.7
Rab11fip1	3.426	1.7
Rnf10	0.000	1.7

B Nanog-siRNA vs GFP-siRNA

Gene	Q value (%)	Fold
Slc40a1	1.046	5.3
Bhmt	1.486	3.4
Klhl13	1.046	3.0
Q9D3E4	1.046	2.8
Spink3	1.824	2.7
Mup5	2.636	2.6
Bmp8b	2.154	2.5
Sms	0.249	2.5
Ap3b2	0.288	2.3
Ctgf	0.000	2.3
Rnpepl1	2.636	2.2
Dpp4	2.636	2.2
Wt1	0.000	2.1
Tm6sf1	0.000	2.1
Fabp5	0.288	2.1
Ly6f	0.249	2.1
Glrx2	0.922	2.1
Zbp1	0.249	2.1
Gm600	3.158	2.1
Cth	2.636	2.1
Stra8	1.737	2.0
Rnf32	0.288	2.0
H19	0.000	2.0
Slc16a14	0.000	2.0
Saa3	0.288	2.0
Gadd45g	2.154	2.0
Irgm	0.288	2.0
Gbp4	0.922	2.0
Otx2	0.288	1.9
Acyp2	0.288	1.9

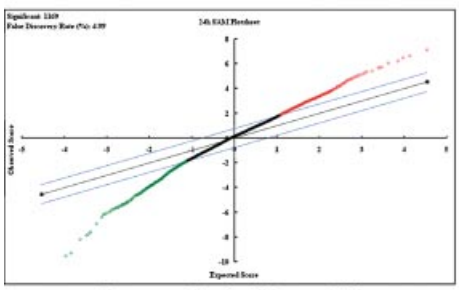

Gene	Q value (%)	Fold
Il1rap	0.000	15.0
Trim10	0.210	10.3
Dlgh2	0.000	9.4
Insl5	0.000	8.5
Dusp23	0.000	8.2
Olfr951	0.000	8.2
Tmem81	0.000	7.5
Hist1h2bb	0.659	6.6
Itgbl1	0.210	6.5
Zik1	1.049	6.2
Olfr663	0.724	4.8
Cd200r3	0.000	4.5
Q8BV22	1.762	4.5
Hs2st1	0.000	4.3
Epgn	1.049	4.3
Olfr1031	1.049	3.8
Sgcb	0.000	3.8
Slc41a3	1.198	3.7
Slamf9	0.000	3.7
Aebp1	0.000	3.7
Smox	0.000	3.5
Pcsk6	0.659	3.4
Zfp54	3.426	3.3
Rnasel	2.761	3.2
Neurod2	2.586	3.0
Plvap	1.198	2.8
Q9D2L2	3.965	2.8
Crhbp	2.586	2.7
Chchd5	0.000	2.7
Nanog	0.000	2.6

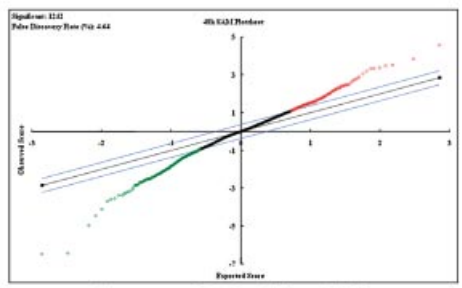

Gene	Q value (%)	Fold
Olfr663	0.000	34.5
Il1rap	0.000	21.7
Hist1h2bb	0.371	20.8
Trim10	0.000	20.8
Itgbl1	0.000	17.0
Insl5	0.439	15.1
Dlgh2	0.000	14.2
Olfr105	0.371	12.5
Rnasel	0.000	10.2
Q8BV22	0.922	9.7
Olfr951	0.371	8.4
Zik1	1.046	8.0
Dusp23	0.000	8.0
Sgcb	0.000	7.6
Plvap	0.371	6.2
Tmem81	0.000	5.0
Hs2st1	0.000	4.3
Trpc4	1.046	4.3
Neurod2	0.000	4.0
Pcsk6	0.000	4.0
Cd200r3	0.000	3.9
Serpinb9f	0.000	3.9
Smox	0.000	3.7
Sesn3	1.046	3.4
Zfp54	1.737	3.3
Klk1	0.000	3.0
Nanog	0.000	2.9
Ccl25	0.439	2.9
Slamf9	0.855	2.8
Cox15	0.439	2.6

Fig. 5. SAM analysis of gene expression profile in Nanog-silencing cells. Top 30 differentially regulated genes with fold change in the significant different genes at 24 h (**A**) and 48 h (**B**) after Nanog-silencing. Only known genes are listed. [Color figure can be viewed in the online issue, which is available at www.interscience.wiley.com.]

and Idb1 (Fig. 4B) [Fujikura et al., 2002; Ahn et al., 2004; Vernay et al., 2005; Tabibzadeh and Hemmati-Brivanlou, 2006]. Aes1 was previously identified as a target gene of STAT3 in mouse ES cells [Sekkaï et al., 2005]. Tcf3 was involved in Wnt signaling pathway and Id1 was the downstream target of BMP4 [Molenaar et al., 1996; Ying et al., 2003; Miyabayashi et al., 2007]. Utf1 and Otx2 were related with Oct4 in ES cells [Saijoh et al., 1996; Matoba et al., 2006; Babaie et al., 2007]. Leftb (Lefty 1) was previously considered as a marker of stemness, but its expression was not quenched upon differentiation. The expression of Lefty 1 increased following ES cells differentiation induced by retinoic acid (RA) or LIF removed [Sekkaï et al., 2005; Tabibzadeh and Hemmati-Brivanlou, 2006]. All of these suggested complex regulatory network in which Nanog and other factors (STAT3, Oct4, Wnt, and Bmp4) collectively regulated downstream genes to control ES cell differentiation. These factors formed a regulatory network to regulate each other, which maintain the properties of ES cells. GATA6, a known differentiated marker gene, was also reported as a downstream target gene of Nanog [Chambers et al., 2003]. Its expression was repressed by Nanog in ES cells and ICM. When Nanog was downregulation or ES cells differentiation, GATA6 expression can be upregulated. In our experiment, GATA6 was also upregulated when Nanog was knockdown. Patterns of expression for these genes are all shown in Figure 4B.

We also analyzed genes involved in signaling pathways according to their expression during Nanog downregulation (Table II). We observed significant changes in key components of Notch, MAPK, Jak-STAT3, Wnt, TGFβ, and cell cycle signaling pathway. This finding was consistent with previous report that these signaling pathways may be involved in mouse ES cells differentiation and pluripotency [Niwa et al., 1998; Jirmanova et al., 2002; Ying et al., 2003; Sato et al., 2004].

Comparison With Previous Analyses

Recently, genome-wide surveys of Nanog and Oct4-binding sites have been performed on human ES cells by chromatin–immunoprecipitation-on-chip assays (ChIP-Chip) [Boyer et al., 2005] and on mouse ES cells by ChIP-PET assays [Loh et al., 2006]. The study of Boyer is an initial step in deciphering the network of transcription factors that regulate ES cells self-renewal. They found that Nanog was associated with 1,687 of the promoter regions in the −8 to +2 kb region, relative to the transcription start site [Boyer et al., 2005]. In Loh's paper, 1,531 genes were identified as direct downstream target of Nanog in mouse ES cells [Loh et al., 2006]. In our experiment, Nanog expression was acutely downregulated in J1 cells using RNA interference, and then expression profiling was analyzed by cDNA microarray to identify potential downstream targets of Nanog. We then compared our result with the result by Loh, which was also obtained from mouse ES cell (Fig. 6). In 1,169 genes, 902 genes had unigene name. A portion of 146 out of 902 genes (16%) in our study overlapped with Loh's ChIP-PET result (supplemental online data Table III). These overlapping genes might be the direct target genes of Nanog. Other genes that were either up- or downregulated on Nanog knockdown but unavailable in the data set of Loh may be considered as the indirect target or novel target genes of Nanog (Fig. 6).

TABLE II. Signaling Pathways of Which Gene Components Show Significant Expression Changes When Nanog was Silenced

Pathway name	Total genes	*P* value
Aminosugars metabolism	6	0.0000
Gap junction	12	0.0000
B cell receptor signaling pathway	7	0.0000
Notch signaling pathway	5	0.0000
Long-term potentiation	7	0.0000
Cell communication	8	0.0000
Insulin signaling pathway	9	0.0000
MAPK signaling pathway	18	0.0000
Carbon fixation	5	0.0000
Regulation of actin cytoskeleton	15	0.0000
Phosphatidylinositol signaling system	6	0.0000
Jak-STAT signaling pathway	10	0.0000
Focal adhesion	14	0.0000
Cell cycle	12	0.0000
Antigen processing and presentation	12	0.0000
Fructose and mannose metabolism	5	0.0011
Calcium signaling pathway	8	0.0015
Arginine and proline metabolism	5	0.0015
Cytokine–cytokine receptor interaction	13	0.0016
Wnt signaling pathway	8	0.0018
TGF-beta signaling pathway	6	0.0019
Glycolysis/gluconeogenesis	5	0.0019
Cell adhesion molecules (CAMs)	8	0.0022
Apoptosis	6	0.0027
mTOR signaling pathway	4	0.0066

Conformation of Gene Expression by Real-Time PCR

To validate the data of microarray, we performed real-time PCR with specific primers to confirm relative changes in the expression

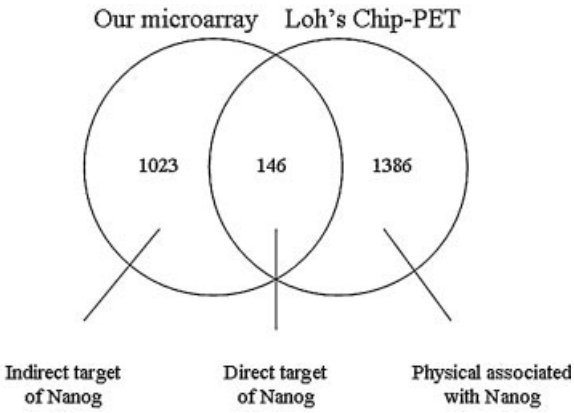

Fig. 6. The VENN diagram shows overlaps between genes differentially expressed in Nanog-silencing ES cells and published direct targets based on ChIP-PET. The region of overlap between our and Loh's result indicated the number of direct target genes of Nanog. Nonoverlapping region in our result indicate indirect target genes or novel target genes of Nanog.

level of some genes. Eighteen genes were chosen for validation by quantitative real-time PCR analysis. Our primers sequences were listed in supplemental online data Table I. Values for each gene were normalized to value obtained for GAPDH. All of these genes showed a comparable alteration between microarray assay and real-time PCR analysis as shown in Figure 7. Although real-time PCR analysis showed greater sensitivity and dynamic range than that of microarray experiments, the data obtained from two methods showed the same positive or negative trend (Fig. 7).

DISCUSSION

It is widely recognized that gain- and loss-of-function approaches are essential for understanding the function of specific genes. RNA interference provides a new approach for elucidation of gene function. RNAi is a sequence-specific, post-transcriptional gene silencing mechanism initiated in animals and plant by the introduction of double stranded RNA homologous in sequence to the silenced genes [Bass, 2001; Elbashir et al., 2001]. In this work, we generated Nanog knockdown ES cells using RNA interference. Barriers to achieving efficient and specific gene silencing in RNAi experiment include limitations in transfection efficiency and specificity of RNAi silencing effectors [Elbashir et al., 2002]. The impact of poor transfection efficiency on RNAi knockdown is significant. In our experiment, we used Cy3 to observe the transfection efficiency. The results demonstrated that nearly 93% of cells are successfully transfected and this transfection efficiency was sufficient for our RNAi experiment. Off-target effects could be corrected by GFP-siRNA control [Cullen, 2006].

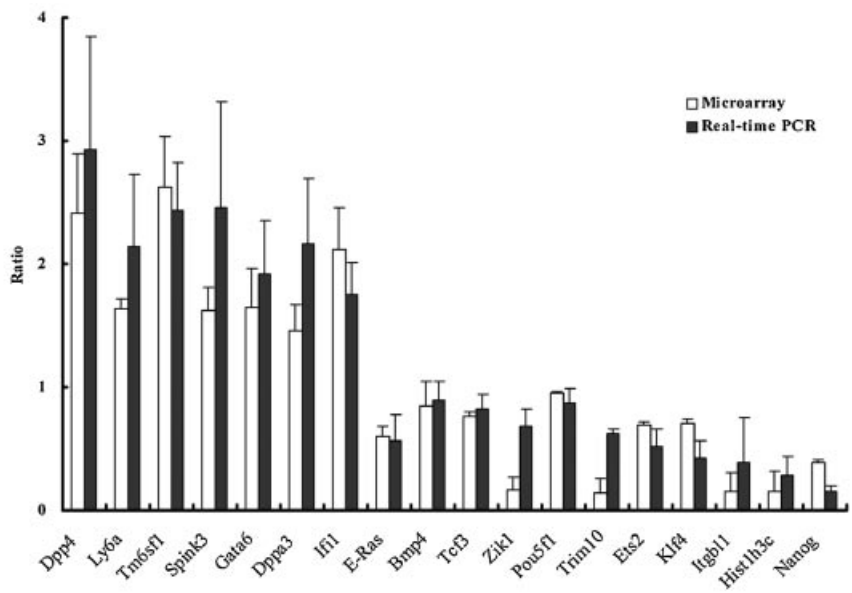

Fig. 7. Real-time PCR confirmed our microarray result. Eighteen genes were chosen for validation by quantitative real-time PCR analysis. All of these genes showed a comparable alteration between microarray assay and real-time PCR analysis.

It has been reported that Nanog expression can be downregulated using RNAi method in ES cells [Hyslop et al., 2005; Zaehres et al., 2005; Hough et al., 2006]. In those reports retroviral and lentiviral vectors or other vectors were used to suppress Nanog expression for long time. Nanog downregulation induced ES cells differentiation. Gene expression pattern was changed following ES cells differentiation. Most of these changed genes might be the result of differentiation following with Nanog-silencing. To narrow down this signature and to enrich it for genes that are likely targets of Nanog, we focused on genes changed immediately after Nanog was suppressed using duplex short RNA (dsRNA) in vitro. At 24 h (earlier time point for Nanog downregulation), we observed the change of gene expression by microarray. At this time point, Nanog expression level in Nanog-silencing cells was significantly lower than control cells (Fig. 1). But Oct4 expression level showed no significant change in Nanog-silencing ES cells compared with control, indicating J1 cells had no significant differentiation when Nanog-siRNA-P1 was transfected for 24 h. But, at this time point, undifferentiated transcription factor 1 (Utf1), a very reliable marker for early differentiation, was obviously decreased. Utf1 was regarded as a sensitive marker of undifferentiated ES cells. Importantly, its transcriptional regulation was very sensitive to differentiation cues and switched off faster and with a larger magnitude than Oct4 or Sox2 during ES cells differentiation [Tan et al., 2007]. The expression pattern of Oct4 and Utf1 indicated that Nanog downregulation could induce ES cells differentiation. Twenty-four hours after Nanog was silenced, the differentiation was switched on, but the differentiation-related genes expression had no significant change. At this time point, less effect of differentiation was included in our result. Here, 1,169 genes were identified as the potential target genes of Nanog in mouse ES cells. These changed genes in our experiment were considered as the result of Nanog downregulation, and this would help us to known better the mechanism of Nanog in ES cells.

Nanog is a crucial factor for maintaining ES cell pluripotency. A first step to understand the function of Nanog is to identify downstream target genes. Two groups have provided a list of Nanog target genes by analysis of their regulatory sequences (such as enhancers/promoters) which can be bound by Nanog using ChIP-Chip in human ES cells and ChIP-PET in mouse ES cells. They showed some important information about how Nanog regulated ES cells self-renewal and differentiation. But many crucial questions remained unanswered. First, their results could not provide us enough information about the positive or negative effect of Nanog on these genes. Second, Nanog regulate genes expression not only by direct effect (bound to enhancers/promoters) but also by the indirect effect. Results from Boyer and Loh could not give us information about the indirect target genes of Nanog. Furthermore, promoters of some genes could bind with Nanog, but did not mean they were regulated by Nanog [Boyer et al., 2005; Orkin, 2005; Loh et al., 2006; Matoba et al., 2006]. Such information can be obtained only by analyzing of global gene expression profiling when Nanog expression was specifically and acutely altered in ES cells. Our result based on RNA interference and microarray analysis could provided more information about the Nanog regulation network in ES cells pluripotency and early differentiation. To better evaluate the relationship between Nanog and these target genes, we compared our result with Loh's, which was also obtained from mouse ES cells. 146 genes out of 1,169 were overlap with Loh's result [Loh et al., 2006]. We considered this part of genes as the direct targets of Nanog, such as GATA6, Tcf3, Ets2, Utf1, Otx2, and others. Nanog bound the promoter of these genes and regulated their expression. The remaining genes that were either up- or downregulated with Nanog knockdown but were unavailable in the data set of Loh might be the indirect target or novel target genes of Nanog. All of the 1,169 changed genes seemed to be involved in the effect of Nanog on ES cells pluripotency. This information provided new sight to understand the mechanism of Nanog in ES cells self-renewal and early differentiation.

Our results indicate that RNA interference combined with microarray method is a feasible and effective approach to identify genes involved in Nanog regulation pathway. The approaches used in this work can be applied to other key transcription factors functioning in ES cells. The results presented here further our understanding of the mechanisms of Nanog in ES cells. Further functional analysis of these

identified genes is required to better understand the molecular mechanism of Nanog in ES cells self-renewal. However, our work has shed new light on the mechanisms underlying the function of Nanog in ES cells. The meaningful information obtained here about ES cells self-renewal and differentiation will be beneficial for other investigator in this filed.

ACKNOWLEDGMENTS

This study was supported by National Natural Science Foundation of China (30570357 and 30600238) and Tianjin Municipal Science and Technology Commission (06YFSZSF01300 and 05YFJZJC01500).

REFERENCES

Ahn JI, Lee KH, Shin DM, Shim JW, Lee JS, Chang SY, Lee YS, Brownstein MJ, Lee SH, Lee YS. 2004. Comprehensive transcriptome analysis of differentiation of embryonic stem cells into midbrain and hindbrain neurons. Dev Biol 265:491–501.

Avilion AA, Nicolis SK, Pevny LH, Perez L, Vivian N, Lovell-Badge R. 2003. Multipotent cell lineages in early mouse development depend on SOX2 function. Genes Dev 17:126–140.

Babaie Y, Herwig R, Greber B, Brink TC, Wruck W, Groth D, Lehrach H, Burdon T, Adjaye J. 2007. Analysis of Oct4-dependent transcriptional networks regulating self-renewal and pluripotency in human embryonic stem cells. Stem Cells 25:500–510.

Bass BL. 2001. RNA interference, the short answer. Nature 411:428–429.

Boyer LA, Lee TI, Cole MF, Johnstone SE, Levine SS, Zucker JP, Guenther MG, Kumar RM, Murray HL, Jenner RG, Gifford DK, Melton DA, Jaenisch R, Young RA. 2005. Core transcriptional regulatory circuitry in human embryonic stem cells. Cell 122:947–956.

Cartwright P, McLean C, Sheppard A, Rivett D, Jones K, Dalton S. 2005. LIF/STAT3 controls ES cell self-renewal and pluripotency by a Myc dependent mechanism. Development 132:885–896.

Chambers I, Colby D, Robertson M, Nichols J, Lee S, Tweedie S, Smith A. 2003. Functional expression cloning of Nanog, a pluripotency sustaining factor in embryonic stem cells. Cell 113:643–655.

Cullen BR. 2006. Enhancing and confirming the specificity of RNAi experiments. Nat Methods 3:677–681.

Daheron L, Opitz SL, Zaehres H, Lensch WM, Andrews PW, Itskovitz-Eldor J, Daley GQ. 2004. LIF/STAT3 signaling fails to maintain self-renewal of human embryonic stem cells. Stem Cells 22:770–778.

Darr H, Mayshar Y, Benvenisty N. 2006. Overexpression of NANOG in human ES cells enables feeder-free growth while inducing primitive ectoderm features. Development 133:1193–1201.

Eisen MB, Spellman PT, Brown PO, Botstein D. 1998. Cluster analysis and display of genome-wide expression patterns. Proc Natl Acad Sci USA 95:14863–14868.

Elbashir SM, Harborth J, Lendeckel W, Yalcin A, Weber K, Tuschl T. 2001. Duplexes of 21-nucleotide RNAs mediated RNA interference in cultured mammalian cells. Nature 411:494–498.

Elbashir SM, Harborth J, Weber K, Tuschl T. 2002. Analysis of gene function in somatic mammalian cells using small interfering RNAs. Methods 26:199–213.

Evans MJ, Kaufman MH. 1981. Establishment in culture of pluripotential cells from mouse embryos. Nature 292: 154–156.

Fujikura J, Yamato E, Yonemura S, Hosoda K, Masui S, Nakao K, Miyazaki Ji J, Niwa H. 2002. Differentiation of embryonic stem cells is induced by GATA factors. Genes Dev 16:784–789.

Hamazaki T, Kehoe SM, Nakano T, Terada N. 2006. The Grb2/Mek pathway represses Nanog in murine embryonic stem cells. Mol Cell Biol 26:7539–7549.

Hough SR, Clements I, Welch PJ, Wiederholt KA. 2006. Differentiation of mouse embryonic stem cells after RNA interference-mediated silencing of OCT4 and Nanog. Stem Cells 24:1467–1475.

Hyslop L, Stojkovic M, Armstrong L, Walter T, Stojkovic P, Przyborski S, Herbert M, Murdoch A, Strachan T, Lako M. 2005. Downregulation of NANOG induces differentiation of human embryonic stem cells to extraembryonic lineages. Stem Cells 23:1035–1043.

Ivanova N, Dobrin R, Lu R, Kotenko I, Levorse J, DeCoste C, Schafer X, Lun Y, Lemischka IR. 2006. Dissecting self-renewal in stem cells with RNA interference. Nature 442: 533–538.

Jirmanova L, Afanassieff M, Gobert-Gosse S, Markossian S, Savatier P. 2002. Differential contributions of ERK and PI3-kinase to the regulation of cyclin D1 expression and to the control of the G1/S transition in mouse embryonic stem cells. Oncogene 21:5515–5528.

Kielman MF, Rindapää M, Gaspar C, van Poppel N, Breukel C, van Leeuwen S, Taketo MM, Roberts S, Smits R, Fodde R. 2002. Apc modulates embryonic stem-cell differentiation by controlling the dosage of beta-catenin signaling. Nat Genet 32:594–605.

Li E, Bestor TH, Jaenisch R. 1992. Targeted mutation of the DNA methyltransferase gene results in embryonic lethality. Cell 69:915–926.

Li Y, McClintick J, Zhong L, Edenberg HJ, Yoder MC, Chan RJ. 2005a. Murine embryonic stem cell differentiation is promoted by SOCS-3 and inhibited by the zinc finger transcription factor Klf4. Blood 105:635–637.

Li ZJ, Wang ZZ, Zheng YZ, Xu B, Yang RC, Scadden DT, Han ZC. 2005b. Kinetic expression of platelet endothelial cell adhesion molecule-1 (PECAM-1/CD31) during embryonic stem cell differentiation. J Cell Biochem 95: 559–570.

Li J, Wang G, Wang C, Zhao Y, Zhang H, Tan Z, Song Z, Ding M, Deng H. 2007. MEK/ERK signaling contributes to the maintenance of human embryonic stem cell self-renewal. Differentiation 75:299–307.

Liu N, Lu M, Tian X, Han Z. 2007. Molecular mechanisms involved in self-renewal and pluripotency of embryonic stem cells. J Cell Physiol 211:279–286.

Loh YH, Wu Q, Chew JL, Vega VB, Zhang W, Chen X, Bourque G, George J, Leong B, Liu J, Wong KY, Sung KW, Lee CW, Zhao XD, Chiu KP, Lipovich L, Kuznetsov VA, Robson P, Stanton LW, Wei CL, Ruan Y, Lim B, Ng HH. 2006. The Oct4 and Nanog transcription network

regulates pluripotency in mouse embryonic stem cells. Nat Genet 38:431–440.
Matoba R, Niwa H, Masui S, Ohtsuka S, Carter MG, Sharov AA, Ko MS. 2006. Dissecting Oct3/4-regulated gene networks in embryonic stem cells by expression profiling. PLoS ONE 1:e26.
Matsuda T, Nakamura T, Nakao K, Arai T, Katsuki M, Heike T, Yokota T. 1999. STAT3 activation is sufficient to maintain an undifferentiated state of mouse embryonic stem cells. EMBO J 18:4261–4269.
Meissner A, Wernig M, Jaenisch R. 2007. Direct reprogramming of genetically unmodified fibroblasts into pluripotent stem cells. Nat Biotechnol 25:1177–1181.
Mitsui K, Tokuzawa Y, Itoh H, Segawa K, Murakami M, Takahashi K, Maruyama M, Maeda M, Yamanaka S. 2003. The homeoprotein Nanog is required for maintenance of pluripotency in mouse epiblast and ES cells. Cell 113:631–642.
Miyabayashi T, Teo JL, Yamamoto M, McMillan M, Nguyen C, Kahn M. 2007. Wnt/beta-catenin/CBP signaling maintains long-term murine embryonic stem cell pluripotency. Proc Natl Acad Sci USA 104:5668–5673.
Molenaar M, van de Wetering M, Oosterwegel M, Peterson-Maduro J, Godsave S, Korinek V, Roose J, Destrée O, Clevers H. 1996. XTcf-3 transcription factor mediates beta-catenin-induced axis formation in Xenopus embryos. Cell 86:391–399.
Nichols J, Zevnik B, Anastassiadis K, Niwa H, Klewe-Nebenius D, Chambers I, Schöler H, Smith A. 1998. Formation of pluripotent stem cells in the mammalian embryo depends on the POU transcription factor Oct4. Cell 95:379–391.
Niwa H, Burdon T, Chambers I, Smith A. 1998. Self-renewal of pluripotent embryonic stem cells is mediated via activation of ST AT3. Genes Dev 12:2048–2060.
Niwa H, Miyazaki J, Smith AG. 2000. Quantitative expression of Oct-3/4 defines differentiation, dedifferentiation or self-renewal of ES cells. Nat Genet 24:372–376.
Okita K, Ichisaka T, Yamanaka S. 2007. Generation of germline-competent induced pluripotent stem cells. Nature 448:313–317.
Orkin SH. 2005. Chipping away at the embryonic stem cell network. Cell 122:828–830.
Paling NR, Wheadon H, Bone HK, Welham MJ. 2004. Regulation of embryonic stem cell self-renewal by phosphoinositide 3-kinase-dependent signaling. J Biol Chem 279:48063–48070.
Pan G, Pei D. 2005. The stem cell pluripotency factor NANOG activates transcription with two unusually potent subdomains at its C terminus. J Biol Chem 280: 1401–1407.
Patterson TA, Lobenhofer EK, Fulmer-Smentek SB, Collins PJ, Chu TM, Bao W, Fang H, Kawasaki ES, Hager J, Tikhonova IR, Walker SJ, Zhang L, Hurban P, de LF, Fuscoe JC, Tong W, Shi L, Wolfinger RD. 2006. Performance comparison of one-color and two-color platforms within the MicroArray Quality Control (MAQC) project. Nat Biotechnol 24:1140–1150.
Pereira L, Yi F, Merrill BJ. 2006. Repression of Nanog gene transcription by Tcf3 limits embryonic stem cell self-renewal. Mol Cell Biol 26:7479–7491.
Reubinoff BE, Pera MF, Fong CY, Trounson A, Bongso A. 2000. Embryonic stem cell lines from human blastocysts: Somatic differentiation in vitro. Nat Biotechnol 18:399–404.
Saijoh Y, Fujii H, Meno C, Sato M, Hirota Y, Nagamatsu S, Ikeda M, Hamada H. 1996. Identification of putative downstream genes of Oct-3, a pluripotent cell-specific transcription factor. Genes Cells 1:239–252.
Sato N, Meijer L, Skaltsounis L, Greengard P, Brivanlou AH. 2004. Maintenance of pluripotency in human and mouse embryonic stem cells through activation of Wnt signaling by a pharmacological GSK-3-specific inhibitor. Nat Med 10:55–63.
Sekkaï D, Gruel G, Herry M, Moucadel V, Constantinescu SN, Albagli O, Tronik-Le Roux D, Vainchenker W, Bennaceur-Griscelli A. 2005. Microarray analysis of LIF/Stat3 transcriptional targets in embryonic stem cells. Stem Cells 23:1634–1642.
Silva J, Chambers I, Pollard S, Smith A. 2006. Nanog promotes transfer of pluripotency after cell fusion. Nature 441:997–1001.
Smith A. 1998. Cell therapy: In search of pluripotency. Curr Biol 8:R802–R804.
Smith AG, Heath JK, Donaldson DD, Wong GG, Moreau J, Stahl M, Rogers D. 1988. Inhibition of pluripotential embryonic stem cell differentiation by purified polypeptides. Nature 336:688–690.
Tabibzadeh S, Hemmati-Brivanlou A. 2006. Lefty at the crossroads of "stemness" and differentiative events. Stem Cells 24:1998–2006.
Takahashi K, Yamanaka S. 2006. Induction of pluripotent stem cells from mouse embryonic and adult fibroblast cultures by defined factors. Cell 126:663–676.
Takahashi K, Tanabe K, Ohnuki M, Narita M, Ichisaka T, Tomoda K, Yamanaka S. 2007. Induction of pluripotent stem cells from adult human fibroblasts by defined factors. Cell 131:861–872.
Tan SM, Wang ST, Hentze H, Dröge P. 2007. A UTF1-based selection system for stable homogeneously pluripotent human embryonic stem cell cultures. Nucleic Acids Res 35:e118.
Tusher V, Tibshirani R, Chu G. 2001. Significance analysis of microarrays applied to the ionizing radiation response. Proc Natl Acad Sci USA 98:5116–5121.
Van Gelder RN, von Zastrow ME, Yool A, Dement WC, Barchas JD, Eberwine JH. 1990. Amplified RNA synthesized from limited quantities of heterogeneous cDNA. Proc Natl Acad Sci USA 87:1663–1667.
Vernay B, Koch M, Vaccarino F, Briscoe J, Simeone A, Kageyama R, Ang SL. 2005. Otx2 regulates subtype specification and neurogenesis in the midbrain. J Neurosci 25:4856–4867.
Watanabe S, Umehara H, Murayama K, Okabe M, Kimura T, Nakano T. 2006. Activation of Akt signaling is sufficient to maintain pluripotency in mouse and primate embryonic stem cells. Oncogene 25:2697–2707.
Wernig M, Meissner A, Foreman R, Brambrink T, Ku M, Hochedlinger K, Bernstein BE, Jaenisch R. 2007. In vitro reprogramming of fibroblasts into a pluripotent ES-cell-like state. Nature 448:318–324.
Williams RL, Hilton DJ, Pease S, Willson TA, Stewart CL, Gearing DP, Wagner EF, Metcalf D, Nicola NA, Gough NM. 1988. Myeloid leukaemia inhibitory factor maintains the developmental potential of embryonic stem cells. Nature 336:684–687.

Yang YH, Dudoit S, Luu P, Lin DM, Peng V, Ngai J, Speed TP. 2002. Normalization for cDNA microarray data: A robust composite method addressing single and multiple slidesystematic variation. Nucleic Acids Res 30:e15.

Ying QL, Nichols J, Chambers I, Smith A. 2003. BMP induction of Id proteins suppresses differentiation and sustains embryonic stem cell self-renewal in collaboration with ST AT3. Cell 115:281–292.

Yoshida K, Chambers I, Nichols J, Smith A, Saito M, Yasukawa K, Shoyab M, Taga T, Kishimoto T. 1994. Maintenance of the pluripotential phenotype of embryonic stem cells through direct activation of gp130 signalling pathways. Mech Dev 45:163–171.

Yu J, Vodyanik MA, Smuga-Otto K, Antosiewicz-Bourget J, Frane JL, Tian S, Nie J, Jonsdottir GA, Ruotti V, Stewart R, Slukvin II, Thomson JA. 2007. Induced pluripotent stem cell lines derived from human somatic cells. Science 318:1917–1920.

Zaehres H, Lensch MW, Daheron L, Stewart SA, Itskovitz-Eldor J, Daley GQ. 2005. High-efficiency RNA interference in human embryonic stem cells. 23:299–305.